PRAMANA
— journal of
physics

© Indian Academy of Sciences

Vol. 65, No. 4
October 2005
pp. 601–614

Self-organized structures in soft confined thin films

ASHUTOSH SHARMA
Department of Chemical Engineering, Indian Institute of Technology,
Kanpur 208 016, India
E-mail: ashutos@iitk.ac.in

Abstract. We present a mini-review of our recent work on spontaneous, self-organized creation of mesostructures in soft materials like thin films of polymeric liquids and elastic solids. These very small scale, highly confined systems are inherently unstable and thus self-organize into ordered structures which can be exploited for MEMS, sensors, opto-electronic devices and a host of other nanotechnology applications. In particular, mesomechanics requires incorporation of intermolecular interactions and surface tension forces, which are usually inconsequential in classical macroscale mechanics. We point to some experiments and quasi-continuum simulations of self-organized structures in thin soft films which are germane not only to nanotechnology, but also to a spectrum of classical issues such as adhesion/debonding, wetting, coatings, tribology and membranes.

Keywords. Soft thin film; dewetting; patterning; adhesion; mesoscale mechanics; self-organization.

PACS Nos 68.35.Gy; 47.20.Ma; 47.54.+r; 82.35.Gh

1. Introduction

Polymeric micro- and nanostructures and patterns are of direct relevance in a wide spectrum of technological applications including antireflective and stealth coatings, micro- and nanoelectromechanical systems (MEMS and NEMS), masks and sacrificial layers in silicon-based electronics, lab-on-a-chip small sensors, and in the rapidly coming age of polymer-based opto-electronics including displays. Thin (<100 nm) liquid and polymer films are ubiquitous in our daily lives in a variety of settings, ranging from agricultural sprays adhering to leaves, coatings and paints, to the film of tears which protects the cornea of the eye. Thin films are also critical in a wide spectrum of technological and scientific applications such as mineral recovery by floatation, food, cosmetics, petrochemical and pharmaceutical foams and emulsions. Further, the problem of stability and spontaneous pattern formation in thin (∼100 nm) films is central to a scientific understanding of a host of physical and biological nanoscale phenomena such as wetting, adhesion, friction, debonding, heterogeneous nucleation, colloids, membrane-morphology and the influences of interfaces and confinement on such classical 'bulk' phenomena as diffusion, phase-separation and phase change. It must however be remembered that in addition to

the creation (or destruction) and mechanical stability of structures, other mesoscale properties such as opto-electronic, catalytic, thermal and chemical properties may be intimately tied to the final applications of these structures, but are quite beyond the scope of this presentation.

There are several challenges in the mechanical behavior, properties and crafting of mesoscale structures using soft materials like polymers, which often necessitate entirely different chemistry, physics, engineering and manufacturing paradigms from the more familiar ones in the relatively mature technology of hard materials like metals and silicon. There are now a variety of soft-lithography techniques in use and many more are being developed at a furious pace. These 'standard' techniques are not reviewed here. The scope of this article is limited to a mini-summary of the efforts of my group at IIT Kanpur over the past five years [1–20] in the understanding, manipulation, control and creation of small polymer structures by self-organization without the use of standard techniques such as photolithography. Although one often thinks of the 'bottom-up' or 'top-down' approaches in engineering of small structures, self-organization is, strictly speaking, neither! Self-organization refers to the spontaneous shape-changes or shaping of material brought about by the inherent stability and dynamics of the system itself. Thus, compared to other techniques, exploitation of self-organization as a patterning tool requires a more fundamental scientific understanding of the physics, chemistry and mechanics of materials so as to tailor a desired pattern from a myriad of potentialities.

2. Stability and intermolecular forces in liquid films

The initial processing of soft materials like polymers in the creation of thin coatings and devices is often in liquid form (solution or melt), which allows inexpensive, flexible and fast approaches to manufacturing. Permanent solid structures are then developed by strategies such as solvent evaporation, cross-linking or cooling of the melt.

Small scale (<100 nm), highly confined soft (shear modulus <10 MPa) structures are inherently unstable or metastable [1–20] because of their high surface energy and because proximal interfaces are able to 'communicate' with each other by various types of intersurface forces such as the electrostatic force, and by (integrated) intermolecular interactions such as the 'long-range' van der Waals force, structural forces of various hues and the 'acid–base' interactions. The intersurface forces decay with the distance between the surfaces. The stability, adhesion failure and defects formation in thin (<100 nm) liquid structures depend crucially on the long-range intermolecular forces that can cause significant deformations of soft interfaces.

In order to facilitate the discussion that follows, a very brief consistent summary of the key theoretical results about the stability, morphology and dynamics of thin films is given. The long wave ($\lambda \gg h$) equation of evolution for a non-slipping, isothermal, single component, Newtonian fluid film without evaporation/condensation on a physically or chemically rough substrate is obtained from the Navier–Stokes equation as follows [3,6,8,15]:

$$3\mu h_t + [(h-af)^3\{\gamma(h_{xx}+h_{yy})-\phi\}_x]_x + [(h-af)^3\{\gamma(h_{xx}+h_{yy})-\phi\}_y]_y = 0, \quad (1)$$

where subscripts denote differentiation; $h(x, y, t)$ is the local film height measured from a datum, $z = 0$; $z = af(x, y)$ describes a rough substrate surface; μ is the viscosity, γ is the surface tension; and the intermolecular potential, ϕ, is a function of the local film thickness, $\eta = [h(x, y, t) - af(x, y)]$, where $\eta = h$ on a smooth surface.

The gradient of potential, $-\phi_x$ (or $-\phi_y$) causing the surface deformations can be written as the sum of forces on the film surface arising from two different mechanisms:

$$\phi_x = (\partial\phi/\partial h)(\partial h/\partial x) + \partial\phi/\partial x|_h. \quad (2)$$

The first term represents the force due to a change in the potential with a change in the local thickness, and the condition for spinodal instability is a negative 'spinodal parameter', $(\partial\phi/\partial h) < 0$ (negative diffusivity). The second term is the force due to change in the potential (at a constant film thickness) because of the physical and chemical heterogeneities of the substrate ($\phi = \phi(x)$; figure 1d) that engender different interactions with the film at different locations, x. Under the action of this force, the fluid moves to maximize its interactions. Simply put, fluid moves from the less wettable to the more wettable sites, thus causing deformations of the free surface. This mechanism of surface deformation (which may frequently also lead to dewetting) is distinct from the spinodal dewetting, and will be referred to as 'heterogeneous instability' or 'heterogeneous dewetting' [6,8,13–16]. The condition for heterogeneous dewetting is that the (destabilizing) potential contrast generated by the heterogeneity must overcome the stabilizing effect of surface tension or the energy penalty for surface deformation. Depending on the film thickness, this requires a critical size and 'strength' of the heterogeneity, and thus the concept of heterogeneous dewetting is akin to 'nucleation'. In a spinodally unstable film on a heterogeneous substrate, both modes of instability compete, but the latter becomes increasingly more important and effective as the film thickness increases and the spinodal parameter becomes weak ($\partial\phi/\partial h \to 0$) [6,8,13–16,18].

It is important to note that the potential for an unstable film is always made up of antagonistic (attractive and repulsive) interactions with different rates of decay with distance (short and long range) [1]. No surface instability is possible in the absence of an attractive force, while no study of dewetting/contact angle is possible within the hydrodynamic framework unless there is a dominant short-range repulsion near the substrate. Unless there is a physical reason to expect a short-range van der Waals repulsion such that $\phi \to +\infty$ as $\eta \to 0$, a 'contact' repulsion like (B/η^9) has to be included to remove the (nonphysical) singularity at $\eta \to 0$. A general representation of the potential is thus (C_i can be positive or negative; positive sign in ϕ denotes destabilizing influence due to attraction and negative sign denotes stabilizing influence due to repulsion):

$$\phi = C_1 f_1(\eta) + C_2 f_2(\eta) + \cdots, \quad (3)$$

where $f(\eta)$ represent the decay behavior of interactions ($\sim 1/\eta^3$ for van der Waals). The most popular representations of the potential for unstructured thin (<10 nm)

films (for example, simple liquids and amorphous polymers) that also respect the underlying physics are ($B > 0$) [1–3,6,8,11,13–18]:

$$\phi = (A_s/6\pi\eta^3) - (S_p/l_p)\exp(-\eta/l_p) - (B/\eta^9), \tag{4}$$

$$6\pi\phi = \left[\frac{(A_s - A_{c1})}{(\eta + d_{c1} + d_{c2})^3} + \frac{(A_{c1} - A_{c2})}{(\eta + d_{c2})^3} + \frac{A_{c2}}{\eta^3}\right] - (B/\eta^9), \tag{5}$$

where A_s denotes the effective Hamaker constant for the van der Waals interaction with a semi-infinite thick substrate (for example, silicon); its positive and negative values denote long-range attraction (possibility of van der Waals force driven instability) and repulsion, respectively. S_p in eq. (4) denotes the strength of a medium-range attraction ($S_p < 0$) or repulsion ($S_p > 0$) with l_p being its correlation (decay) length. In addition to the substrate interaction, eq. (5) also takes into account the possibility of van der Waals interactions of the film with two successive thin coatings of the substrate with thicknesses d_{c1} and d_{c2} and their net Hamaker constants, A_{c1} and A_{c2}, respectively. For example, a nonwettable ($A_{c1} > 0$) oxide layer of thickness d_{c1} on a wettable ($A_s < 0$) silicon substrate, followed by an adsorbed or grafted layer of polymer of thickness d_{c2} provides a soft near-surface repulsion ($A_{c2} > 0$).

For thicker (>10 nm) films, retardation of van der Waals force makes it much weaker and also changes its decay to $\sim 1/\eta^4$ instead of $1/\eta^3$. Another way to look at retardation is to define an effective Hamaker constant in eqs (4) and (5) that is a function of thickness. Defined this way, the effective Hamaker constant is already reduced by a factor of about 2 for a 5 nm thick film, and by about an order of magnitude for a 10 nm film. Although retardation is a well-known fact, it needs repeating since it is often overlooked in the attempts to fit the length- and time-scales of instability in thin films and in 'reconciliation' of forces based on length-scale arguments.

Equations (4) and (5) with appropriate signs of the Hamaker constants (A_s, A_{c1}, A_{c2}) and S_p can represent the generic variation of the spinodal parameter shown in figure 1C, and more. In particular, eq. (5) (with $d_{c2} = 0$; $A_s < 0$ and $A_{c1} > 0$) has been found useful for fitting the experiments for the low M_w PS films on oxide covered silicon wafers. PDMS films under water [4,5] are represented by the curve in figure 1C. A chemically heterogeneous substrate either has different forms of potential in different regions or the parameters of a potential (A, S_p and the substrate coating thicknesses, d_{c1}, d_{c2}) vary along the substrate. Thus ϕ on a heterogeneity is different from its surroundings, thus resulting in a force, ϕ_x, on the liquid.

On a homogeneous smooth surface, where $a = 0$ and $\partial\phi/\partial x|_h = 0$, the linear stability analysis of eq. (1) gives the short time or initial length-scale of instability, λ (or the number density of features, N), and the time-scale for the appearance of first hole (where ε is the initial small amplitude; $\varepsilon \ll h$) [1–5,16]:

$$\lambda = [-8\pi^2\gamma/(\partial\phi/\partial h)]^{1/2}; \quad N = \lambda^{-2} = -(\partial\phi/\partial h)/8\pi^2\gamma, \tag{6}$$

$$\tau = 12\mu\gamma[h^3(\partial\phi/\partial h)^2]^{-1}\ln(h/\varepsilon). \tag{7}$$

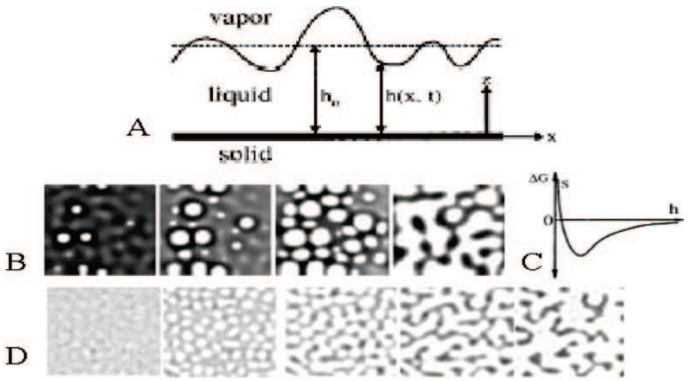

Figure 1. Stages of spontaneous dewetting in a relatively thick film by the formation of holes. (**A**) Schematic of thin film instability, (**B**) simulations, (**C**) potential for the thin film, (**D**) experiments on a (∼40 nm) PDMS (silicon oil) film sandwiched between a silicon wafer and water.

The above equations, which predict $\lambda \sim h^2$ and $\tau \sim h^5$ for a nonretarded van der Waals potential, are the most widely used forms for interpretation of thin-film stability and for the determination of potential from measurements of λ. These equations are a good first guide when the conditions leading to eq. (1) are met in an experiment, $\varepsilon \to 0$ and the thickness is deep inside the spinodal territory where $(\partial\phi/\partial h)$ is not vanishingly small [16]. However, in general, for any finite initial amplitude, eq. (1) has to be solved directly for the actual (nonlinear) length- and time-scales and the film morphology, which can differ significantly for finite amplitudes.

Thus, understanding the mechanics at small scales requires a direct quantification of intersurface forces that cannot be directly measured for a soft deformable surface by any known technique, including the atomic force microscopy (AFM). The latter is suitable only for the measurement of forces between two hard surfaces. We have suggested a new technique [4,5,16], thin film force microscopy (TFFM), for a direct measurement of interaction energies ($\sim kT$) by using the general principle that deformation of a surface, and the resulting structures, contain the unique signature of the force.

As an example of this technique, figure 1 summarizes the major events in the time-evolution of patterns in a relatively thick film (∼40 nm) [3–5]. Figure 1D illustrates a typical experiment on the spontaneous rupture and dewetting of a thin (<50 nm) silicon oil film under water on a smooth silicon wafer (a process which is also involved in the cleaning of surfaces or detergency). Several holes open up in the film, expand and coalesce to transform the oil film into a large number of tiny droplets. In essence, attractive intersurface forces grow stronger with a decline in the local thickness, which engenders the surface instability and deformation of the free surface of the film by causing a flow from the thinner to the thicker regions. The underlying physics of thin film dewetting is thus similar to the spinodal phase separation where a negative diffusivity facilitates movement from low concentration to high concentration. Figure 1C shows our computer simulations [3], of the same process based on the equations of motion in which intersurface

forces (and their decay with local film thickness) are incorporated. Interestingly, based on the linear stability analysis or simulations, it is possible to correlate the number of holes/droplets per unit area to the intersurface force and thus, to resolve the problem of characterization of the nanoscale interactions based directly on the facile observations of the thin-film morphology. In essence, a stronger attractive force engenders a stronger instability manifested in a higher density of holes and droplets per unit area. A particularly simple relation between the number density (N) and the intermolecular force per unit volume (ϕ) is [1–3]: $N = \phi/8\pi^2\gamma$, where γ is the surface tension of the film. Thus, by counting the number of droplets resulting from dewetting of different thickness films, we were able to directly measure the magnitude and decay of long-range van der Waals force [$\phi(h) \sim h^{-4}$] in a thin liquid film. In essence, dewetting pattern becomes a 'thin-film force microscope' to peer into the highly enigmatic realm of the intermolecular forces!

Interestingly, the results [3–5,16] show that the van der Waals forces (per unit area), which at 100 nm are considered to be already four to five orders of magnitude weaker than the atmospheric pressure, can cause significant, measurable, macroscopic changes in short times at distances of hundreds of nanometers in very viscous (∼10,000 water viscosity) films! Thus, although one thinks of the van der Waals forces as mere weaklings, these can gather enough collective muscle by cooperation of a large number of molecules. These results have far-reaching consequences in the entire area of colloids and interfaces, and in their virtually limitless applications in both the physico-chemical and biological domains.

There are two major lessons from the above example: (a) nanoscale soft structures are not always mechanically stable but can be destabilized by the long-range intermolecular forces and (b) the length-scale of structure caused by the instability can be used to quantify the magnitude and decay behavior of intermolecular forces. In fact, a dominant dogma of thin films until as late as the mid-nineties (!) held that the circular holes witnessed in spontaneous dewetting are caused by nucleation by defects such as heterogeneities, dirt particles, cavities, etc. On the contrary, the spontaneous dewetting by intermolecular forces, when ordained by thermodynamics, cannot be prevented without significant interfacial engineering. A technological implication is the conventional remedies, such as cleaning and polishing the substrates, and the preparation of film in clean rooms, will not stop a thin film from self-destructing! However, a more controlled, directed dewetting can in fact be turned to advantage to engineer small structures as discussed in the next section.

However, as one moves closer to the critical thickness where $(\partial\phi/\partial h) = 0$, the density of structures and their morphology show far greater sensitivity to the amplitude and wave number of the initial conditions and eqs (6) and (7) are no longer adequate [16]. This is because the linear time-scale diverges, $\tau \sim (\partial\phi/\partial h)^{-2} \to \infty$ near h_C, but the actual (nonlinear) time, depending on the local amplitude, is far shorter. Thus, local small depressions (even of say 2% amplitude) can quickly grow into holes that expand to occupy some of the space where the other potential holes of the linear theory could eventually have manifested. Also, clustering of holes by the formation of secondary holes around the initial holes becomes more prominent toward the critical point. Some of the interesting morphological aspects (as well as the statistical aspects) are best illustrated with the help of a large domain 3D

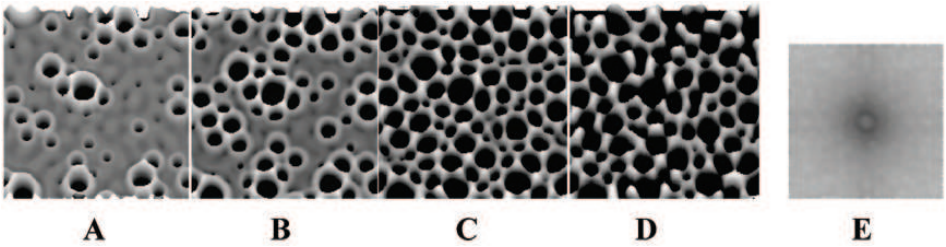

Figure 2. Simulated time evolution (**A** → **D**) of instability in a 5.5 nm film (critical thickness beyond which the film is stable is 6.8 nm). Simulation shows a $10\lambda \times 10\lambda$ domain, starting from a random roughness of 1% maximum amplitude at initial time. **E** shows the Fourier transform of **C** confirming the isotropy of the structure and the linear theory expectation for its length-scale. The maximum number of holes (in **C**) are 93, as compared to the linear theory prediction of 100 holes in this domain of size $100\lambda^2$. A shift in the bi-modal hole size distribution to a wide mono-modal distribution over time (**A** → **C**) is also reminiscent of experimental patterns obtained by freezing the evolution at different times in evaporating collagen films (figures 1a and 1c of U Thiele, M Mertig and W Pompe, *Phys. Rev. Lett.* **80**, 2869 (1998)).

simulation that can clearly resolve the larger structures and their distributions at longer times. Figure 2 presents one such case from our study for the development of pattern in a 5.5 nm thick film starting with a random small amplitude (1% of thickness) roughness [16]. For the potential chosen here, a 5.5 nm thick film is in the twilight zone between the better behaved deep spinodal territory ($<\sim$5 nm) and the defect sensitive spinodal regime as one approaches critical thickness (6.8 nm). Indeed, the evolution has signatures of both regimes in that the length- and time-scales from the nonlinear simulation are quite close to the linear theory predictions, but the structure evolves by the formation of a small population of primary holes around which a larger number of secondary 'satellite' holes begin to develop. Another interesting aspect is a distinctly bi-modal distribution of hole sizes in the early stages of evolution before all the holes have formed, but a later shift towards the mono-modal distribution although with a wide variance. This is because the growth of primary holes is nearly arrested after the formation of satellite holes. An important point is that unless relatively large-amplitude local defects are present, the length- and time-scales of the structure may continue to be 'well-behaved' even though the morphological evolution appears somewhat unorthodox [16].

Further discussion about the 'Defect Sensitive Spinodal Regime' may be found elsewhere [16].

3. Gaining control: Patterning by directed dewetting on heterogeneous substrates or 'templates'

Is it possible to gain control of the disordered dewetting process for producing ordered mesoscale structures for technological applications? What would be the conditions and triggers necessary for the creation of such structures by self-organization? Self-organization, which is the art of gently persuading the system

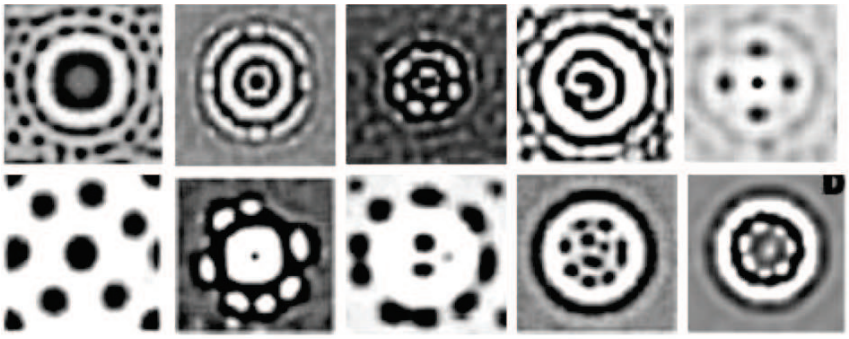

Figure 3. Various types of locally ordered patterns generated around different types of localized physico-chemical substrate heterogeneities [6,8,13–15,18].

along the desired goals by knowing its 'mind', entails much less 'violence' inherent in the conventional 'top-down' methods of microstructure creation such as micro-machining, photolithography, etc. requiring several complex and expensive steps.

Interestingly, controlled dewetting on a chemically or physically patterned substrate (that can be tailored by conventional lithographies or self-assembly methods) can produce a variety of self-organized, highly ordered patterns [6,8,13–16,18]. In essence, a heterogeneous substrate causes a gradient of chemical potential (force) that moves the fluid molecules from the less wettable (higher energy) to more wettable (lower energy) regions. Our simulations [6,8,15,16] showed (figure 3) that even an isolated heterogeneity can produce a variety of locally ordered structures (layers of satellite holes and droplets, 'ripples', 'flowers', 'castle-moat' structure). Such enigmatic structures 'nucleated' by surface 'defects' are also frequently witnessed in the experiments and illustrate some very interesting physics of microdomain free surface flows.

Using chemical or physical patterns etched onto substrates, called templates, we have theoretically shown that the dewetting can be controlled and manipulated [6,8,13–16,18]. Instead of being a random event, controlled dewetting transforms thin films into well-ordered structures. Understanding the precise conditions under which ordered, complex structures can self-organize on the sub-micron to nanometer scales (one-thousandth to one-millionth of a millimeter) may be of potential use in polymer-based electronic devices, electromechanical systems and sensors of various hues.

The central issue is how faithfully the substrate patterns are reproduced in a thin film spontaneously, i.e., how effective is the templating of soft materials by the dewetting route and what are the conditions for ideal templating? For example, figure 4 displays the different patterns that result by dewetting on a substrate consisting of parallel stripes of alternating wettabilities or potentials. Only a certain combination of film thickness and the template (figure 4b) produces a well-aligned pattern. Similarly, figure 5 summarizes the dewetting morphologies on more complex 2D substrate patterns. All of the well-ordered simulated morphologies shown in figure 5 result only under certain restrictive conditions, but not always [6,8,13–16,18]. Establishing precise conditions for ideal templating takes the guess-

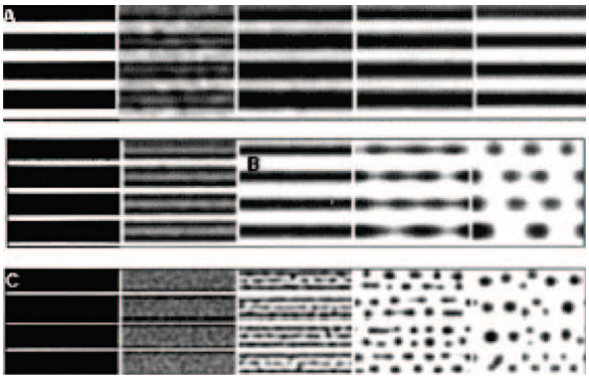

Figure 4. The first gray scale pictures in each row display the substrate pattern (white is nonwettable and black is wettable). The subsequent pictures show time evolution of pattern in thin films coated on these substrates (white = dewetted areas; black = liquid). Only the conditions in A (first row) are conducive for ideal templating or a faithful reproduction of the substrate pattern in the dewetting film [8,13–15].

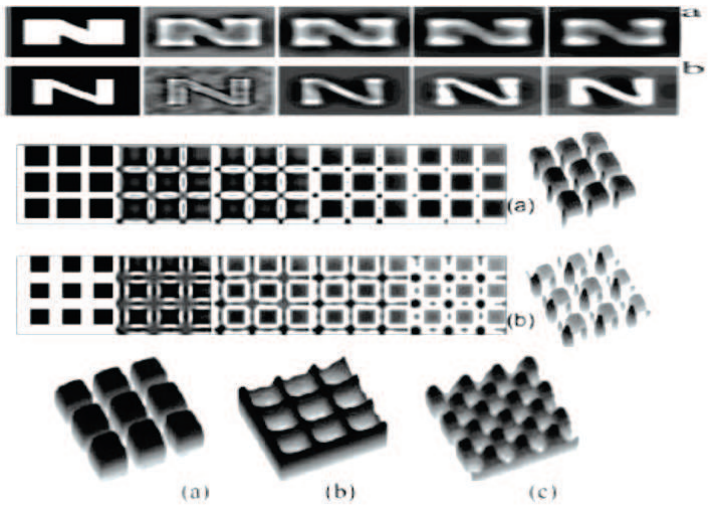

Figure 5. Some examples of simulated structures under conditions of ideal templating. Simulations uncover the conditions for ideal templating of complex ordered patterns by self-organized dewetting on pre-patterned substrates.

work out of many thousands of tedious experiments that have to be otherwise performed to optimize the conditions on the film thickness, materials, and processing conditions. Indeed, several experimental groups have now used the self-organized spontaneous dewetting as a route to mesoscale patterning and have confirmed our theoretical predictions for the conditions for ideal templating.

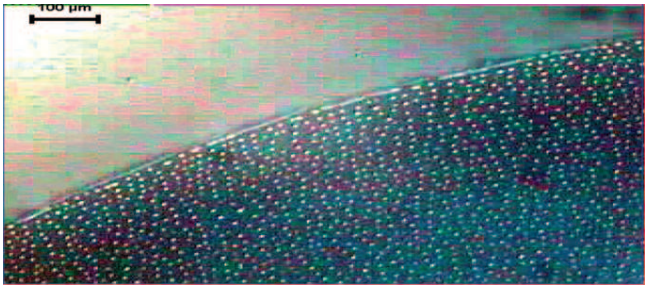

Figure 6. Ordered arrays of polymer droplets obtained by the self-organized contact-line instability of an evaporating polymer solution on quartz.

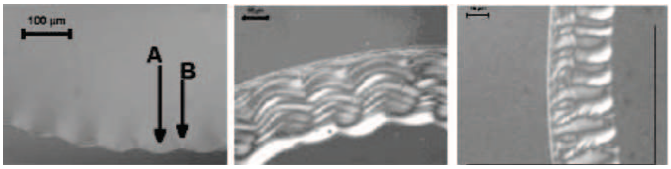

Figure 7. Undulative instability of contact line in an evaporating polymer solution droplet and the resulting polymer structures [20]. The structures form near the initial position of the contact line, the physics of which is akin to the famous 'coffee-stain' effect (a dried coffee drop forms a ring-like stain at its periphery rather than a uniformly distributed circular patch!).

The most important thing is that there is only a narrow window of substrate geometry, size of substrate features, potential contrast and film thickness that leads to ideal templating by circumventing the difficulties hinted above.

4. Self-organized structures by contact line movement during dewetting

The contact line (where liquid meets the substrate) of a dewetting thin film is a nanozone and therefore prone to a variety of instabilities. We have investigated [2,10,12] the instability of the moving contact line and its associated rim in the dewetting of slipping polymer films [17] and polymer solutions [20] on substrates such as silicon wafers and quartz. Small fluctuations near the contact line get spontaneously amplified and produce a periodic self-regulating pattern made up of radially and azimuthally organized features, which may be simple droplets or much more complex. Figures 6 and 7 depict well-aligned polymer droplets and spaghetti features respectively [20], that have been engineered in our laboratory by the evaporation of polymer solutions under optimized set of conditions. Often, the polymer pattern results from a regular undulation of the contact line leading to long finger-like projections, which eventually fragment and reform. As a general theme, nature seems to optimize on the kinetics by sacrificing on the shape by an appropriate self-modulation of the resulting structure.

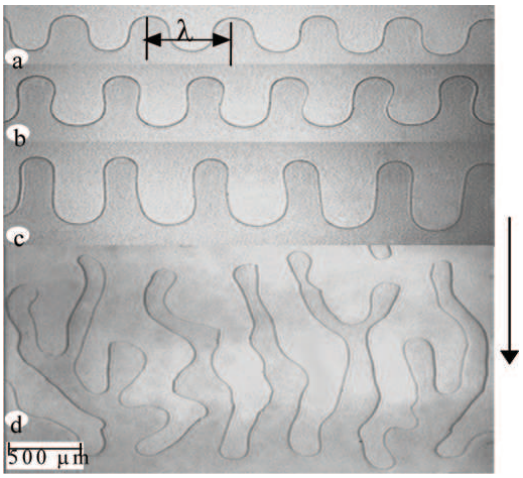

Figure 8. Periodic cracks formed by the contact instability of a thin elastic film by the contact of glass beams. Rigidity of the contactor beam increases from top to bottom, which leaves the wavelength of instability unchanged.

5. Instability and patterning of thin elastic films

How does the behavior of a thin film changes if it is an elastic solid rather than a fluid? For non-Newtonian materials, slippage on the substrate and plastic deformations may also become important. How do they modify the mesoscale mechanics? These questions are also of central importance in our understanding of adhesion, debonding and friction, where interfacial cavitation plays a paramount role.

The general question of what happens when a surface approaches a confined elastic film has been a classical concern of contact mechanics, because it is important for the fundamental understanding of purely elastic instabilities that may ensue without any concurrent mass flow. This issue is also of technological importance in a variety of settings such as the peeling of a pressure-sensitive adhesive from a solid surface, the crazing behavior of glassy polymers, interfacial bonding in composite materials, morphological instability of a biaxially stressed interface in crystal growth situation, elastic surfaces becoming unstable under the action of stresses, and stability of polymer brushes used for improved compatibility. Recently, in collaboration with Vijay Shenoy (now at the Indian Institute of Science, Bangalore), Manoj Chaudhury (Lehigh University, USA) and Animansu Ghatak (currently at IIT Kanpur), we discovered that surfaces of soft solid films, such as rubber, become spontaneously rough when brought in contact with another solid surface [7,9,19]. The microscopic well-ordered cavities thus formed at the interface manifest as long bridges when the two surfaces are pulled apart. The same surface instability modified by viscous element is responsible for the sticky threads that are seen when lady's finger and jackfruit are cut and separated as well as when adhesive is peeled.

We found that the surface of a soft thin elastic film, when brought in contact with another surface, spontaneously develops a rather periodic interfacial instability leading to the formation of interfacial nanocavities and bridges; for example,

as shown in figure 8 [7]. Although it has been historically thought that interfacial cavitation, manifest for example during peeling of an adhesive, is essentially a random phenomenon arising from pre-existing defects, we found a very systematic variation of the number of cavities/bridges per unit area with the film thickness ($N \sim \lambda^{-2} \sim h^{-2}$) [9,19]. Interestingly, and again in contrast with the fluid films, it was also found that the length-scale of surface instability is nearly independent of the material properties such as the shear modulus and the nature of surfaces (type of intersurface forces operative between the contactor and the film! A detailed theoretical analysis [7,19] showed that the instability arises from a competition between the destabilizing intersurface attractive forces such as electrostatic and van der Waals forces and the stabilizing elastic energy opposing deformations. The length-scale of instability is now given by a near universal scaling, $\lambda \sim 3h$, which is in excellent agreement with a variety of experiments [7]. These results have important implications for a potential novel pattern transfer technology based directly on soft solid films rather than on freezing of structures formed in the liquid state. However, unlike the modulation of liquid patterns by an external or intermolecular potential, spontaneous patterning of a thin solid film has far fewer external triggers, the most notable being the film thickness itself.

The patterns and forces that arise as the contacting surface is withdrawn from an elastic film initially in contact can be found based on the search for energy minimizing shapes. Mathematically, this is done by Fourier representing the elastic film shape as follows. If $\mathbf{v}^f$ denotes the displacement vector of the elastic film, the surface deformation of the film normal to the free surface can be represented by

$$v_2^f(x_1, 0) = \sum_{n=0}^{N-1} a_n \cos(k_n x_1).$$

The total energy (sum of intersurface attractive energy and elastic stored energy) is then obtained in terms of Fourier coefficients (film shape) as [19]

$$\Pi = \pi\mu \frac{Lx_1}{2} \sum_{n=0}^{N-1} n a_n^2 k_n \frac{(1 + \cosh(2k_n h) + 2(k_n h)^2)}{(\sinh(2k_n h) - 2k_n h)} + \int_0^{Lx_1} U \left(\sum_{n=0}^{N-1} d + v^p(x_1, d) - a_n \cos(k_n x_1) \right) \mathrm{d}x_1.$$

A conjugate gradient scheme can be employed to search for the Fourier coefficients (a_n) that give the minimum energy at a given separation distance. Equation (1) thus gives the stable equilibrium profile of the film at a given position of the contactor. This methodology resolves several intriguing and fundamental aspects of debonding at soft interfaces, including the formation and persistence of regularly arranged nanocavities and bridges, mechanisms of 'adhesion/debonding hysteresis' and vastly lower adhesive strengths compared to the absence of instability and pattern formation [19]. The analysis shows the hysteresis to be caused by an energy barrier that separates the metastable patterned configurations during withdrawal, and the debonded state. The metastable morphological pathways involving cavitation and peeling of contact zones engender substantially lower debonding forces [19].

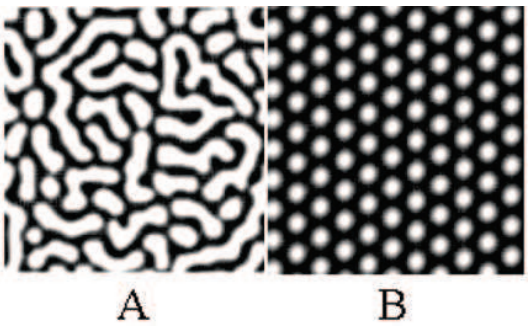

Figure 9. Simulated patterns (also verified experimentally) in thin soft elastic polymer films under different conditions obtained by bringing a rigid flat surface in contact.

Although the elastic contact instability produces a randomly oriented pattern (figure 9A), our recent simulations have shown (figure 9B) that a morphological control of the instability becomes possible by the application of an external electric field near critical conditions for the onset of instability (to be published).

Finally, plastic deformations eventually become important in delamination and debonding of thin solid films, but their consequences have received scant notice in small-scale, highly confined systems. An example is the growth of holes in thin (<100 nm) polymer films below their bulk glass transition temperatures. Since such films have extremely high viscosities, the principal mechanism of deformation appears to be plasticity, rather than viscous flow. Plasticity has interesting consequences in the kinetics and morphology of dewetting, such as exponential hole growth at initial times and decline of velocity at long times [12].

6. Summary

The whole area of interfacial phenomena in highly confined mesoscale systems is buzzing with intense activity worldwide at a feverish pace due to its fundamental scientific implications as well as important technological applications. Confinement simply means that the effects of system size and interactions with its boundaries can have significant qualitative implications for the system behavior, structure and properties. A confined thin film is a highly nonequilibrium situation and various interfacial structures evolve spontaneously to break free of the imposed constraints and confinements. Understanding the response of a thin film to various types of confinements is the key to engineer the desired mesoscale structures by self-organization without complex multi-step conventional silicon or metal-centric methods of patterning, which in any case are not the most suitable techniques for soft materials like the polymers that will become increasingly useful for opto-electronic applications.

As a concluding remark, it is now needed to develop a comprehensive theoretical understanding of mesoscale mechanics for very small (<100 nm), highly confined systems that takes into account essential complexities such as the mechanical material properties (elasticity, yield and plasticity, viscosity, etc.), intermolecular forces

integrated over the system, interfacial tension force, phase change and the boundary behavior such as slippage. This would greatly aid our ability to self-organize soft materials on a hierarchy of length-scales for the creation of useful mesostructures for a variety of applications.

Finally, I would like to point out that due to the space constraints and the nature of this article, much of the discussion is admittedly centered on the recent work of my group, but an interested reader can find relevant references in the articles cited here.

Acknowledgements

It is a special pleasure to thank my past collaborators, students, and associates on thin films whose works have been reported here: They are V Shenoy, M K Chaudhury, G Reiter, A Ghatak, R Khanna, R Konnur, K Kargupta, J Sarkar, M Gonuguntla and S Sarkar.

References

[1] A Sharma, *Langmuir* **9**, 861 (1993)
[2] A Sharma and G Reiter, *J. Colloid Interface Sci.* **178**, 383 (1996)
[3] A Sharma and R Khanna, *Phys. Rev. Lett.* **81**, 3463 (1998)
[4] G Reiter, A Sharma, A Casoli, M-O David, R Khanna and P Auroy, *Langmuir* **15**, 2551 (1999)
[5] G Reiter, R Khanna and A Sharma, *Phys. Rev. Lett.* **85**, 1432 (2000)
[6] R Konnur, K Kargupta and A Sharma, *Phys. Rev. Lett.* **84**, 931 (2000)
[7] A Ghatak, M K Chaudhury, V Shenoy and A Sharma, *Phys. Rev. Lett.* **85**, 4329 (2000)
[8] K Kargupta and A Sharma, *Phys. Rev. Lett.* **86**, 4536 (2001)
[9] V Shenoy and A Sharma, *Phys. Rev. Lett.* **86**, 119 (2001)
[10] G Reiter and A Sharma, *Phys. Rev. Lett.* **87**, 166103 (2001)
[11] A Sharma and J Mittal, *Phys. Rev. Lett.* **89**, 186101 (2002)
[12] V Shenoy and A Sharma, *Phys. Rev. Lett.* **88**, 236101 (2002)
[13] K Kargupta and A Sharma, *J. Chem. Phys.* **116**, 3042 (2002)
[14] K Kargupta and A Sharma, *Langmuir* **18**, 1893 (2002)
[15] K Kargupta and A Sharma, *J. Colloid Interface Sci.* **245**, 99 (2002)
[16] A Sharma, *Euro. Phys. J.* **E12**, 397 (2003)
[17] A Sharma and K Kargupta, *Appl. Phys. Lett.* **83**, 3549 (2003)
[18] K Kargupta and A Sharma, *Langmuir* **19**, 5153 (2003)
[19] J Sarkar, V Shenoy and A Sharma, *Phys. Rev. Lett.* **93**, 018302 (2004)
[20] M Gonuguntla and A Sharma, *Langmuir* **20**, 3456 (2004)